ACS Infectious Diseases

pubs.acs.org/journal/aidcbc Article

6,11-Dioxobenzo[*f*]pyrido[1,2-*a*]indoles Kill *Mycobacterium tuberculosis* by Targeting Iron−Sulfur Protein Rv0338c (IspQ), A Putative Redox Sensor

Rita Székely,[⬡] Monica Rengifo-Gonzalez,[⬡] Vinayak Singh, Olga Riabova, Andrej Benjak, Jérémie Piton, Mena Cimino, Etienne Kornobis, Valerie Mizrahi, Kai Johnsson, Giulia Manina, Vadim Makarov, and Stewart T. Cole*

Cite This: *ACS Infect. Dis.* 2020, 6, 3015−3025 Read Online

ACCESS | Metrics & More | Article Recommendations | Supporting Information

ABSTRACT: Screening of a diversity-oriented compound library led to the identification of two 6,11-dioxobenzo[*f*]pyrido[1,2-*a*]indoles (DBPI) that displayed low micromolar bactericidal activity against the Erdman strain of *Mycobacterium tuberculosis in vitro*. The activity of these hit compounds was limited to tubercle bacilli, including the nonreplicating form, and to *Mycobacterium marinum*. On hit expansion and investigation of the structure activity relationship, selected modifications to the dioxo moiety of the DBPI scaffold were either neutral or led to reduction or abolition of antimycobacterial activity. To find the target, DBPI-resistant mutants of *M. tuberculosis* Erdman were raised and characterized first microbiologically and then by whole genome sequencing. Four different mutations, all affecting highly conserved residues, were uncovered in the essential gene *rv0338c* (*ispQ*) that encodes a membrane-bound protein, named IspQ, with 2Fe−2S and 4Fe-4S centers and putative iron−sulfur-binding reductase activity. With the help of a structural model, two of the mutations were localized close to the 2Fe−2S domain in IspQ and another in transmembrane segment 3. The mutant genes were recessive to the wild type in complementation experiments and further confirmation of the hit−target relationship was obtained using a conditional knockdown mutant of *rv0338c* in *M. tuberculosis* H37Rv. More mechanistic insight was obtained from transcriptome analysis, following exposure of *M. tuberculosis* to two different DBPI; this revealed strong upregulation of the redox-sensitive SigK regulon and genes induced by oxidative and thiol-stress. The findings of this investigation pharmacologically validate a novel target in tubercle bacilli and open a new vista for tuberculosis drug discovery.

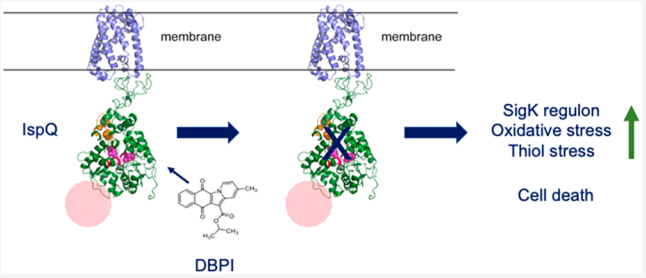

KEYWORDS: *tuberculosis, drug discovery, chemical genomics, iron−sulfur-binding reductase, 6,11-dioxobenzo[f]pyrido[1,2-a]indoles*

Tuberculosis remains a global health problem for which new interventions and therapeutic strategies are sorely needed.[1] Despite intensive efforts, progress toward a broadly efficacious new vaccine remains disappointing, and this reflects not only the magnitude of the challenge but also the complexity of protecting against and killing an intracellular pathogen.[2] For over 60 years, we have been able to curb the etiologic agent *Mycobacterium tuberculosis* by means of short course chemotherapy involving six months of combination therapy.[3,4] However, resistance to two or more of the four front-line agents on which it relies is increasingly common,[1] as is resistance to the second-line drugs which are much less effective and more toxic than their frontline counterparts.[5] This has led to renewed interest in discovering new chemical entities (NCE) to develop as leads for the next generation of tuberculosis drugs, and a variety of approaches have been undertaken to do so.[3] The most effective means of lead generation has been by phenotypic screening of compound libraries for activity against *M. tuberculosis* growing *in vitro*[6] or more recently using host-cell-based screens.[7]

The first new TB drug candidates, bedaquiline,[8] pretomanid,[9] and delamanid,[10] were discovered in the 2000s and are now nearing the end of phase 3 clinical trials.[11] All three new drugs have been approved for the treatment of multidrug resistant tuberculosis (MDR-TB). In the past decade, many additional phenotypic screens were conducted, and these also generated new leads, some of which are currently in early stage clinical trials.[11] However, while there have been some impressive successes, such as the discovery and clinical

Received: July 24, 2020
Published: September 15, 2020

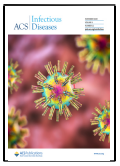

https://dx.doi.org/10.1021/acsinfecdis.0c00531
ACS Infect. Dis. 2020, 6, 3015−3025

Table 1. Structure and MIC of Selected DBPI on *M. tuberculosis* Erdman and H37Rv

Cmpd	Structure	MIC_{99}[a] (μM) by REMA or BacTiter Glo			
		Erdman	Erdman NO Tween	H37Rv	BacTiter
F1414-1444	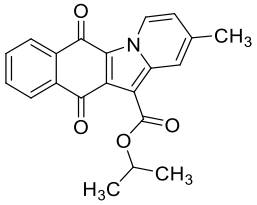	0.85	19.5	1.09	4.68
F1414-1438	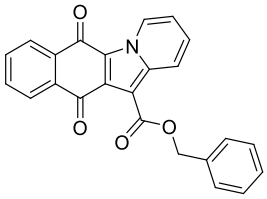	1.1	8.44	2.5	3.2

[a]MIC_{99} is the concentration where 99% of bacterial growth is inhibited.

development of telacebec (Q203),[12] the number of NCE remains relatively limited, and many of them target the same functions in the pathogen. This has led to the notion of the existence of "promiscuous targets" such as DprE1 (decaprenylphosphoryl-β-D-ribose oxidase), MmpL3 (a mycolic acid transporter), and QcrB (the B-subunit of respiratory cytochrome *bc1* complex) that are each inhibited by a wide variety of pharmacophores.[13] Such promiscuity may reflect the bacterial growth conditions used in the screening assays, the limited chemical diversity in the compound collections, or the periplasmic accessibility of the active sites of the targets.[13] In an attempt to explore more chemical space, Switzerland's National Centre of Competence in Research (NCCR) in Chemical Biology established a diversity-oriented library from many different commercial sources to aid the identification of bioactive molecules.[14] In this investigation, we screened the NCCR library and uncovered a new scaffold for drug development, the dioxo-dihydrobenzo-pyridoindoles, and demonstrate that these compounds target an essential yet previously uncharacterized membrane-bound redox enzyme that is likely involved in energy metabolism or redox sensing.

RESULTS AND DISCUSSION

Screening Diversity-Oriented Compound Library. The NCCR (National Centre of Competence in Research) library of 67 393 commercially available compounds was tested for growth inhibition of the Erdman strain of *Mycobacterium tuberculosis* (*Mtb*) using the resazurin reduction microtiter assay (REMA) in a single point (10 μM) screen.[15] This led to the identification of 340 molecules inhibiting growth by >60%. The 66 most active compounds were purchased afresh for hit confirmation and further investigation. Hit confirmation was performed using both the Erdman and H37Rv strains of *Mtb* by the BacTiter-Glo (Promega) and REMA assays to compare their performance in viability testing. The results of both assays showed good correlation, and most of the MICs determined with Erdman were close to those determined with strain H37Rv. Hits were also tested using the following algorithm: REMA with drug susceptible (DS), drug resistant (DR), and multidrug resistant (MDR) clinical and laboratory isolates; REMA with the streptomycin-starved 18b (SS18b) strain of *M. tuberculosis*, a model to find drugs active against nonreplicating bacteria;[16] growth inhibition activity against a range of bacteria and yeast; cytotoxicity (TD_{50}) for HepG2 cells; mutagenicity using the SOS-chromotest;[17] and finally, microsomal stability.

Among the hits, compound F1414−1444 was considered particularly interesting for two reasons. First, a close analogue, F1414−1438, was also found in the primary screen, thus providing the basis for a structure activity relationship (SAR) analysis, and second, because the compound appears to inhibit a new, previously uncharacterized target, as will be described below. Details of the other hits and their targets will be presented elsewhere.

Initial Microbiological Characterization of F1414−1444 and F1414−1438. The two 6,11-dioxobenzo[f]pyrido-[1,2-*a*]indoles (DBPI) analogues, active against the Erdman strain of *M. tuberculosis* in the phenotypic screen of the NCCR compound library, were further characterized by a range of microbiologic and cell-based tests. From Table 1, it can be seen that both DBPI compounds display low micromolar activity in two different assays against the Erdman and H37Rv strains of *M. tuberculosis*, and this activity decreased in the absence of Tween 80, which is known to increase susceptibility to some drugs, such as RIF.[18]

To investigate whether F1414−1444 is bactericidal, we determined its MBC_{99} by incubating bacteria with concentrations of the compound ranging from 0.5−16X MIC for 7 and 14 d in a REMA assay. Dilutions were then spread on 7H10 plates to obtain single colonies. After three weeks' incubation colonies were counted and compared to controls. The MBC_{99} value of F1414−1444 was 1.56 μM, which is close to its MIC_{99}, thus indicating that the compound has bactericidal activity. Furthermore, cidality was found to be time-dependent (Supporting Information Figure S1).

Activity against Nonreplicating Tubercle Bacilli, Clinical Isolates, and Drug-Resistant Laboratory Strains. Strong activity was detected against the streptomycin-starved 18b (SS18b) strain, a model to test drugs against non-replicating bacteria (Table 2), indicating that DBPI should be active against latent tuberculosis. However, while the inhibition

https://dx.doi.org/10.1021/acsinfecdis.0c00531
ACS Infect. Dis. 2020, 6, 3015−3025

Table 2. Activity against SS18

	SS18b	
compound	I_{max} (%)	conc (μM) of I_{max}
F1414−1444	54	23.6
F1414−1438	70	6.4
RIF	60	0.03

[a] I_{max} value represents the highest percent of inhibition.

levels obtained were comparable to those seen with the control drug, RIF, higher concentrations were required.

The susceptibility of five clinical isolates to DBPI compounds was then evaluated by REMA in the presence of Tween. The collection included a fully DS-isolate, three DR-strains and an MDR-strain (Table 3). Both compounds were active against all DR-isolates and the MIC values were in line with those determined using the reference strains (Table 1).

Table 3. Activity against Clinical Isolates and Drug-Resistant Mutants of *M. tuberculosis*[a]

			MIC_{99} (μM)	
isolate/strain	description, genotype	drug resistance	1414−1444	1414−1438
ABG	clinical isolate, pan-susceptible		0.79	4.4
CHUV80045776	clinical isolate, *katG(S315T)*	INH	2.5	3.0
HUG.MB.3649	clinical isolate, *inhA* promoter c(−15)t	INH	2.2	6.5
HUG.MI.1020	clinical isolate, *katG(S315T)*	INH, STR	2.3	2.5
MDR-TB	clinical isolate, *rpoB(S531L)*, *katG(S315T)*	INH, RIF	3.47	2.7
Lsr1	H37Rv *qcrB(L176P)*	lansoprazole	3.0	2.3
Q203-R	H37Rv *qcrB(T313A)*	Q203	2.4	2.5
DR3	H37Rv *mmpL3(V681I, S87P)*	BM212	1.1	2.2
DR5	H37Rv *mmpL3 (G253E, D46G)*	BM212	1.5	5.1
DR6	H37Rv *mmpL3 (V681I, M492T, V564A)*	BM212	1	1.2
DR7	H37Rv *mmpL3(Q40R)*	BM212	0.7	1.1
DR8	H37Rv *mmpL3 (G253E, I516T)*	BM212	0.7	1.2
NTB1	H37Rv *dprE1(C391S)*	BTZ043	7.2	7.4
H37Rv CFZ-R	H37Rv *rv0678(S63R)*	BDQ/CFZ	2.4	2.9

[a] The table is a composite and presents data obtained on different dates. All clinical isolates were tested together, and the other strains were tested later and on several occasions.

To test the possibility that DBPI compounds act on one of the promiscuous targets introduced above, their activity was tested against a panel of drug-resistant mutants of strain H37Rv harboring different mutations in *dprE1*, *mmpL3*, and *qcrB*. In virtually all cases, the DBPI susceptibility of the mutants was close to that of the parental strain H37Rv, thus indicating a new mechanism of action (Table 3). Furthermore, DBPI compounds were also active against a BDQ/CFZ-resistant mutant that overproduces the efflux pump MmpL5 due to a mutation in gene *rv0678* (*mmpR5*).

Activity against Other Bacteria and Yeast. To establish whether F1414−1444 has broad spectrum antimicrobial activity, a collection of various pathogenic and nonpathogenic Gram-positive and Gram-negative bacteria and yeast was assembled and then tested by REMA for DBPI susceptibility (Supporting Information Table S1). Activity was restricted to the *M. tuberculosis* complex and its ancestor *Mycobacterium marinum*. No activity was detected against *Mycobacterium smegmatis*, selected nontuberculous mycobacteria (NTMs), and *Corynebacteria*. The combined results indicate that DBPI compounds have a very narrow range of activity.

Target Identification. Mutants of the Erdman strain resistant to F1414−1444 were raised *in vitro* and characterized by MIC determination and whole genome sequencing (WGS) in an attempt to find the likely target (Table 4). At 3xMIC, mutants arose at a frequency of 3.3×10^{-7}. Irrespective of the level of F1414−1444 used for their selection, all of the mutants were highly resistant, displaying an increase in MIC of 90 to >125-fold (Table 5). Furthermore, all mutants displayed cross-resistance to F1414−1438, thereby indicating that the compounds share the same mechanism of action.

Table 5. Complementation Analysis of F1414−1444-Resistant Mutants

strain	MIC (μM)
Erdman	0.8
DBPI1	100
DBPI2	75
DBPI3	>100
DBPI4	100
Erdman::pMV*E_0374*	0.8
DBPI1::pMV*E_0374*	0.8
DBPI2::pMV*E_0374*	0.8
DBPI3::pMV*E_0374*	0.8
DBPI4::pMV*E_0374*	0.8
Erdman::pMV261	0.8
DBPI1::pMV261	100

All nine mutants were subjected to WGS and bioinformatic analysis and found to harbor polymorphisms in the *ERDMAN_0374* gene, which is identical to *rv0338c* in strain H37Rv, except for a single nucleotide polymorphism (SNP) in

Table 4. WGS Analysis of F1414−1444-Resistant Mutants

number of mutants sequenced	selected at X MIC	relevant SNPs	mutant used elsewhere	domain location	interpro domain[a]
3	3	Asp695Gly	DBPI2	end Cys-rich	IPR004017
1	3	Pro775_Val776 fs	DBPI1	disordered	MOBIDB_LITE
1	10	Gly125Val	DBPI3	TM3	TMHELIX
4	20	Arg641Gly	DBPI4	Cys-rich	IPR004017

[a] Interpro domains from https://www.ebi.ac.uk/interpro/.

https://dx.doi.org/10.1021/acsinfecdis.0c00531
ACS Infect. Dis. 2020, 6, 3015−3025

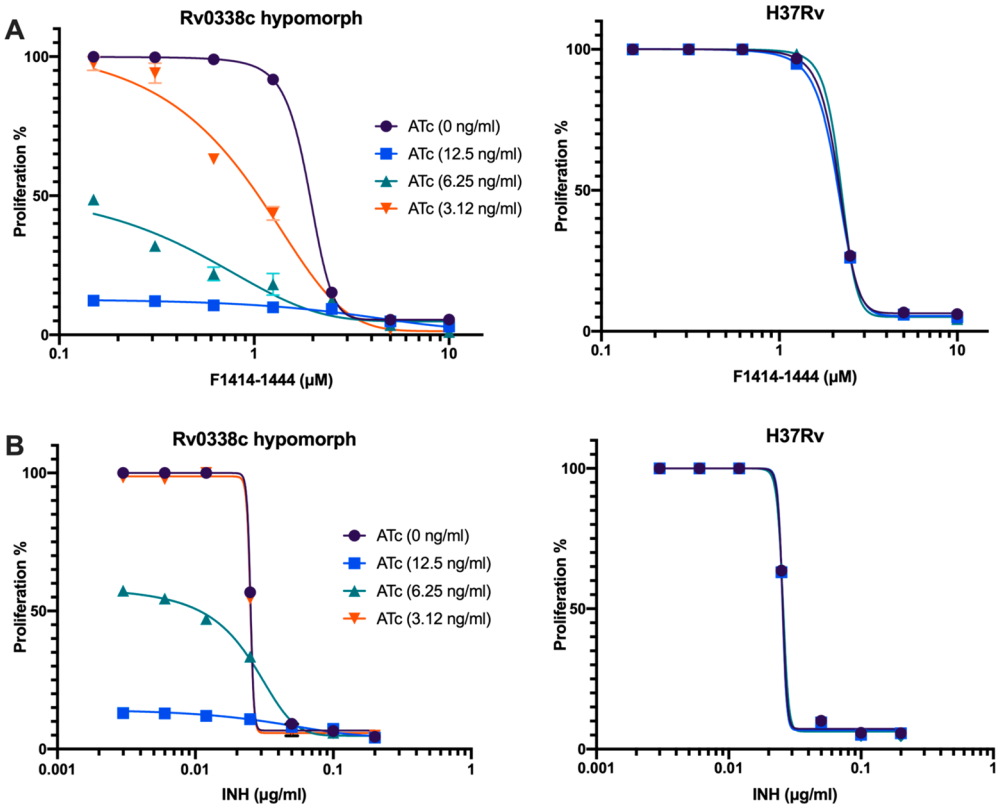

Figure 1. ATc dose-dependent modulation of growth of Rv0338c hypomorph (Rv0338c_Tet-OFF::*attB_rv0337c*) as a function of DBPI concentration. For control purposes, H37Rv was included and grown in the presence or absence of ATc; note the lack of growth inhibition. The conditional knockdown mutant was grown at the ATc concentrations indicated by the color coding in the presence of increasing amounts of (A) F1414−1444 or (B) isoniazid, INH. The data represent mean ± SEM, obtained from at least three biological replicates.

codon 502 that changes Leu to Phe, L502F. The corresponding protein will thus be referred to as Rv0338c or IspQ (iron−sulfur protein Q) henceforth.

From Table 4, it may be seen that two of the mutations (Arg641Gly and Asp695Gly) occurred several times, whereas the others were singletons. To exclude the possibility that these mutations were not DBPI-related, the *rv0338c* sequences in ∼1500 *M. tuberculosis* genomes were inspected.[19] None of the above mutations, nor the Erdman polymorphism, was found, but two SNP were detected, namely G403980A (c.1862C>T), which occurred in ∼99% of the genomes and T404326C (c.1516A>G) occurring in 92% of the cases. These SNP cause the nonsynonymous substitutions Ala621Val and Arg506Gly, respectively. In this set, the Ala621 polymorphism is restricted to 13 strains and isolates, all derived from H37, the parent of H37Rv. Furthermore, Arg506 occurs in 123 genomes that all cluster on the H37Rv "sub-branch" of the branch of *M. tuberculosis* lineage 4. The ancestor of the tubercle bacilli, *M. canettii*, has the Val621/Gly506 duet (see Supporting Information). These amino acid substitutions do not affect susceptibility to DBPI, as indicated by the data reported here, for example the lineage 2 strain, 18b tested above, has the Val621/Gly506 duet as do 92% of the other *M. tuberculosis* complex members.

The *rv0338c* gene has been reported to be essential on the basis of Tn saturation mutagenesis[20] and to encode a putative iron−sulfur containing heterodisulfide reductase,[21] that we have called IspQ for iron−sulfur protein Q.

Target Validation. To confirm that the protein encoded by *rv0338c* plays a role in the mechanism of action of DBPI compounds a genetic approach was applied. The empty pMV261 vector and its pMV*E_0374* construct (i.e., pMV261 carrying the *ERDMAN_0374* gene, equivalent to *rv0338c*) were transformed into the parental Erdman strain and its four representative DBPI-resistant mutants (Table 4). When the parent strain was diploid for *rv0338c*, no change in MIC was observed. However, in the case of all four resistant mutants, complementation with the wild-type gene restored full susceptibility to F1414−1444 (Table 5). In control experiments, transformation of the resistant mutants with the pMV261 vector led to no change in the MIC for F1414−1444. Taken together, the findings provide strong evidence for causality and indicate that the resistant phenotype is recessive when the wild-type gene is present.

Construction and Use of Conditional Knock-Down Mutants. To further investigate the hit−target relationship, we exploited the Tet-Off system as done previously with success for GuaB2, another new drug target in *M. tuberculosis*.[22] To investigate whether F1414−1444 retains target selectivity for IspQ (Rv0338c) in live cells, we asked whether conditional depletion of the protein would sensitize *M. tuberculosis* H37Rv to the growth inhibitory effects of the DBPI compounds. For this purpose, we constructed anhydrotetracycline (ATc)-regulated *rv0338c* conditional knockdown mutants (hypomorphs) in the Tet-OFF configuration, as described recently.[22] The *rv0338c* promoter region was replaced by the ATc-regulated promoter−operator element, $P_{myc1}tetO$, by a single-crossover (SCO) homologous recombination event to generate the promoter-replacement mutant, *rv0338c*-SCO (Supporting Information Figure S2). A

https://dx.doi.org/10.1021/acsinfecdis.0c00531
ACS Infect. Dis. 2020, 6, 3015−3025

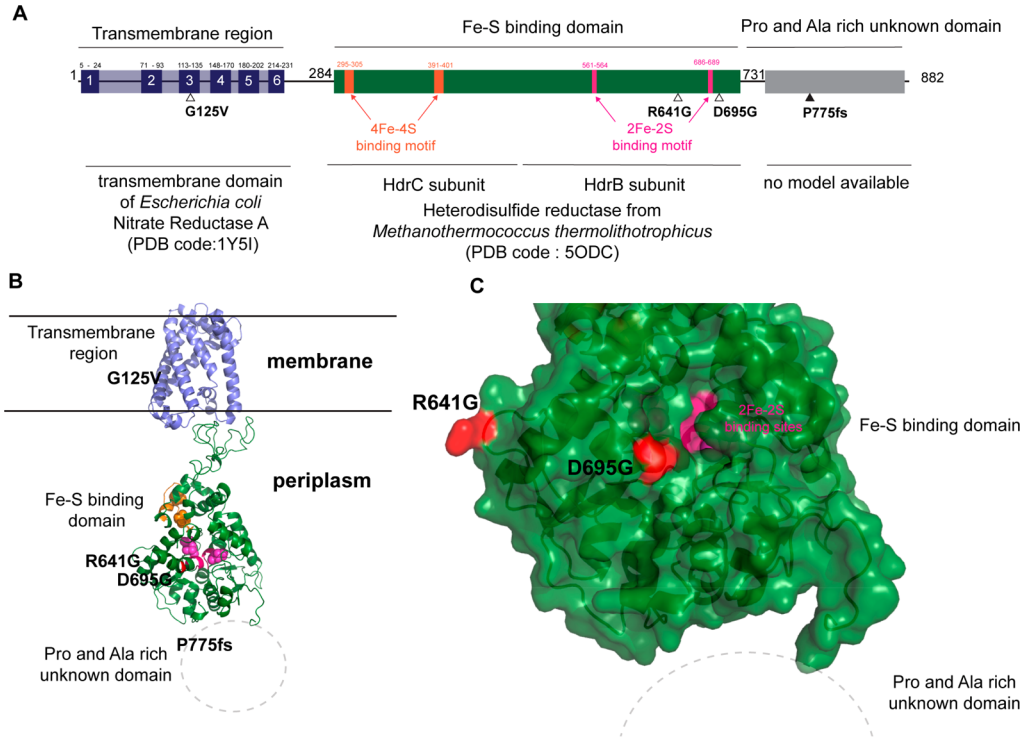

Figure 2. Structural model of IspQ (Rv0338c). (A) The transmembrane domain was modeled using the web server phyre2[24] and the structure of the transmembrane domain of *Escherichia coli* nitrate reductase A subunit as a template.[25] Likewise, the Fe−S binding domains were modeled using as template the structures of the HdrC and HdrB subunits of the heterodisulfide reductase of the archaea *Methanothermococcus thermolithotrophicus*.[26] (B) The orientation and position of the Fe−S domains with respect to the transmembrane domain were arbitrarily chosen in the graphical representation and the C-terminal domain, which could not be modeled, is represented by a gray-dashed circle connected to the C-terminal end of Fe−S domain. (C) Close-up of the entry pocket for the 2Fe−2S site. The side chain of Aspartate 695 is located near the entry of the pocket situated close to the 2Fe−S site (12 Å). The C-terminal part after Pro775 should be located close to this pocket and might impact its structure.

construct bearing the tetracycline repressor was then introduced into *rv0338c*-SCO to obtain a conditional Tet-OFF mutant. Because *rv0337c*, the gene situated 31 bp downstream of *rv0338c*, is also essential, care was taken to avoid potential polar effects on gene expression. Measurement of *rv0337c* mRNA levels by q-PCR in the resistant mutants DBPI1 and DBPI2 (Table 4) revealed these to be about 40−50% of that of the parental strain. Consequently, a second copy of *rv0337c* was introduced into the *attB* site of *rv0338c*-SCO, and the resultant strain Rv0338c_Tet-OFF::*attB_rv0337c* was used for further investigation.

Growth of Rv0338c_Tet-OFF::*attB_rv0337c* in 7H9 medium was inhibited in a dose-dependent manner by ATc, thereby confirming the essentiality of *rv0338c* (Supporting Information Figures S3 and S4) *in vitro*. Next, the conditional knockdown mutant was tested in the checkerboard assay by simultaneously varying the concentrations of ATc and F1414−1444. The results are displayed in Figure 1A, where they are compared to those obtained with an unrelated drug INH (Figure 1B). In the presence of ATc alone at a concentration of 6.25 μg/mL, growth of Rv0338c_Tet-OFF::*attB_rv0337c* was reduced to about 50% of the ATc-free level. Addition of increasing amounts of F1414−1444 or F1414−1438 (Supporting Information Figure S4) led to even slower growth, culminating in >90% inhibition (Figure 1A). A similar but more pronounced trend was observed with 3.12 μg/mL ATc alone, a level that does not impact the growth of the hypomorph as evidenced by its growth curve in the presence of INH (Figure 1B). To illustrate this point, 1 μM F1414−1444 inhibits growth by ∼50% in the presence of 3.12 μg/mL ATc but has no noticeable impact in its absence. The combined data show that as the IspQ level declines, less DBPI is required to inhibit growth, leading us to conclude that IspQ (Rv0338c) is a major DBPI target.

Data Mining, Structural Modeling, and Function Prediction. The Rv0338c/IspQ protein comprises 882 amino acids and is likely to participate in energy production and conversion according to the TubercuList,[21] Interpro (https://www.ebi.ac.uk/interpro/), and COG databases.[23] The N-terminal domain (amino acid residues 1−231), comprising six transmembrane segments (Figure 2, Supporting Information Figure S5), is followed by a [4Fe-4S] ferredoxin-type, iron−sulfur binding domain (residues 279−420, IPR009051), which, in turn, is followed by two cysteine-rich [2Fe−2S] domains (residues 477−568, 607−693). The bulk of the protein (residues 232−882) is predicted to be located in the periplasmic space. Three of the polymorphisms associated with F1414−1444 resistance are nonsynonymous mutations that cause amino acid substitutions, whereas the fourth is a frameshift mutation that will truncate the protein by ∼100 residues (Table 4). The C-terminal domain following the frameshift mutation is proline−alanine-rich, repetitive, and of low complexity and predicted to be intrinsically disordered (Figure 2).

To glean insight into the impact of the four F1414−1444 resistance-associated mutations on IspQ function, a structural model of the protein was built using the web server phyre2[24] and appropriate templates from sequence-related proteins of

https://dx.doi.org/10.1021/acsinfecdis.0c00531
ACS Infect. Dis. 2020, 6, 3015−3025

known structure present in PDB. See legend to Figure 2 for details and additional information.

On inspection of multisequence alignments of IspQ orthologues from various tubercle bacilli, *M. marinum* and *M. smegmatis*, and NTMs positions Gly125, Arg641, Arg695, and Pro775 were all found to be invariant, implying that they may be functionally important. Orthologues of IspQ are also present in the leprosy bacilli *M. leprae* and *M. lepromatosis* with their downsized genomes,[27,28] and again, this is indicative of the biological importance of the protein. However, in the leprosy bacilli, Gly125 has been replaced by Ser, but the other three residues were conserved. In all cases, the most divergent part of the protein is the C-terminal stretch after Pro775, as this appears to be composed of simple sequence repeats that vary in copy number between mycobacterial species (see Supporting Information Figures S3 and S4). Compared to its counterparts in tubercle bacilli, the C-terminal domain of MMAR_0611,[29] the IspQ ortholog of the DBPI-susceptible M strain of *M. marinum* is over 100 amino acids longer due to the expansion of tandem repetitive motifs (see Supporting Information Figure S6).

While the precise biological role of IspQ remains to be elucidated, some information is available about its subcellular location and the regulation of its gene. The protein has been identified in the membrane fraction of *M. tuberculosis* H37Rv by different investigators using mass-spectrometry-based proteomic techniques and notably in Triton X-114 extracts that contain solubilized membrane proteins.[30,31] Being in the plasma membrane, IspQ is ideally located to interact with components of the electron transport chain and lipophilic electron carriers. Consistent with its role as an iron−sulfur protein, expression of *rv0338c* is induced by iron and controlled by IdeR, an iron-dependent regulator.[32]

Transcriptome Analysis. Identifying transcripts whose levels change following exposure of *M. tuberculosis* to drugs or inhibitors is a well-established means of gaining insight into mechanisms of action or resistance.[33] RNA was thus extracted from strain H37Rv that had been exposed to two different concentrations of F1414−1444 or a new analog 11626157 (see next section for details). The latter generally proved the more active. Transcripts whose expression was up- or downregulated by both compounds were identified by RNA-Seq and bioinformatics was then used to glean functional insight (Supporting Table S2). There were many more up- than downregulated genes (Figure 3A), and expression of *rv0338c* was not notably affected by DBPI exposure (Figure 3B).

In both cases, genes associated with the following broad functions were shared: redox reactions, oxidative and thiol stress, and drug efflux (Figure 3B). The most highly induced gene was *mpt70* (*rv2875*), which, together with the linked genes *mpt83*, *dipZ*, *rv2876*, and *rv2877c* is part of the sigma factor K regulon.[34] Expression of other SigK-regulated genes, namely *rv0449c*, *rv0447c*, and *rv0448c*, located adjacent to those for SigK and its antisigma factor, RskA, were also upregulated by 11626157. The basal expression of *mpt70* and *mpt83* in *M. tuberculosis* is low and strongly induced after infection of macrophages[35] and, under reducing conditions, SigK dissociates from RskA to transcribe genes involved in the regulation of redox homeostasis and the serodominant antigens Mpt70 and Mpt83.[36]

Exposure to the two DBPI compounds also led to induction of sets of functionally unrelated genes required for arginine biosynthesis (*argBCDFGJR*),[37] electron transfer and energy production (*cydBCD*),[38] and metalation of secreted proteins (CtpC) such as the manganese-requiring superoxide dismutase, SodA.[39,40] All of these functions are induced by oxidative stress, as is the RND protein MmpL6 that seemingly enables the more virulent, modern epidemic strains of *M. tuberculosis* to resist such stress.[41,42] A second RND protein, MmpL5, and its partner MmpS5, were also upregulated by DBPI, but because MmpL5 exports many drugs, this is most likely a resistance mechanism.[43−45] From Table 3, it may be seen that the MmpL5 overproducer, strain H37Rv CFZ-R, is susceptible to both DBPI compounds tested. MmpL6 expression is upregulated by triclosan and plumbagin, which cause oxidative stress, and presence of the complete *mmpS6 mmpL6* locus can also confer INH and rifampin tolerance to some strains of *M. tuberculosis*.[42]

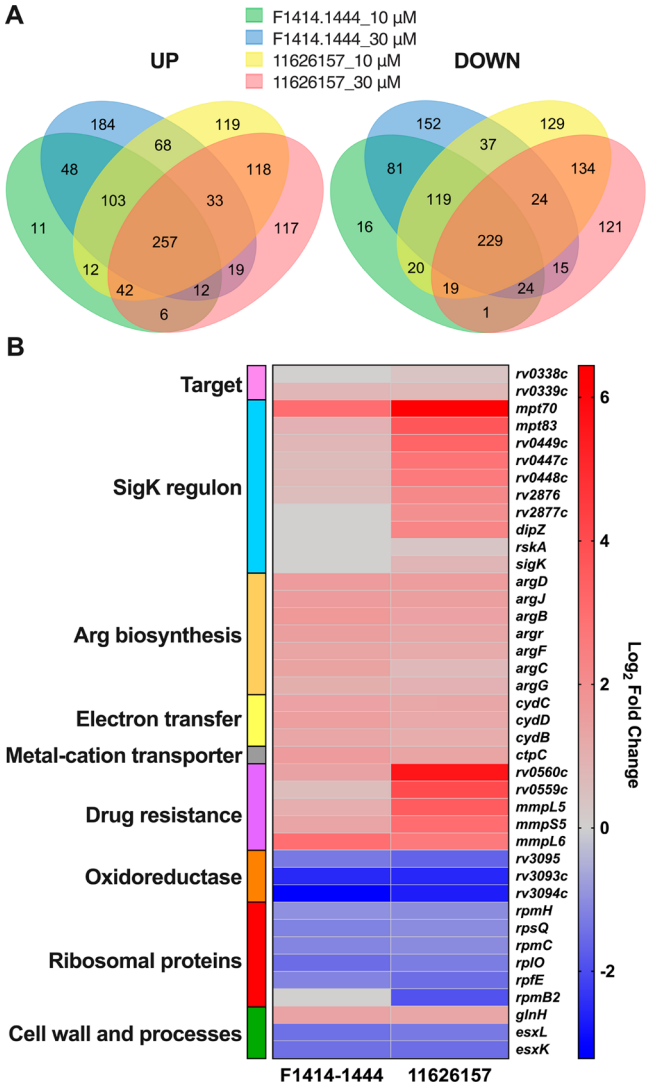

Figure 3. Gene expression profiling in response to F1414−1444 and 11626157. (A) Venn diagrams showing the number of genes significantly up- or downregulated between two different concentrations of the two DBPI compounds (color-coded) and DMSO. (B) The heat map shows genes whose expression was up- or downregulated in red and blue, respectively, according to a $\log_2$ scale. Gray bars indicate singletons that were induced by one or other DBPI but not by both. Preference is given to genes whose expression was most strongly affected by both DBPI or that are functionally related. Functional information is from http://tuberculist.epfl.ch/.

https://dx.doi.org/10.1021/acsinfecdis.0c00531
ACS Infect. Dis. 2020, 6, 3015−3025

Scheme 1. Synthetic Route for 12-*R*-Benzo[*f*]pyrido[1,2-*a*]indole-6,11-dione Derivatives

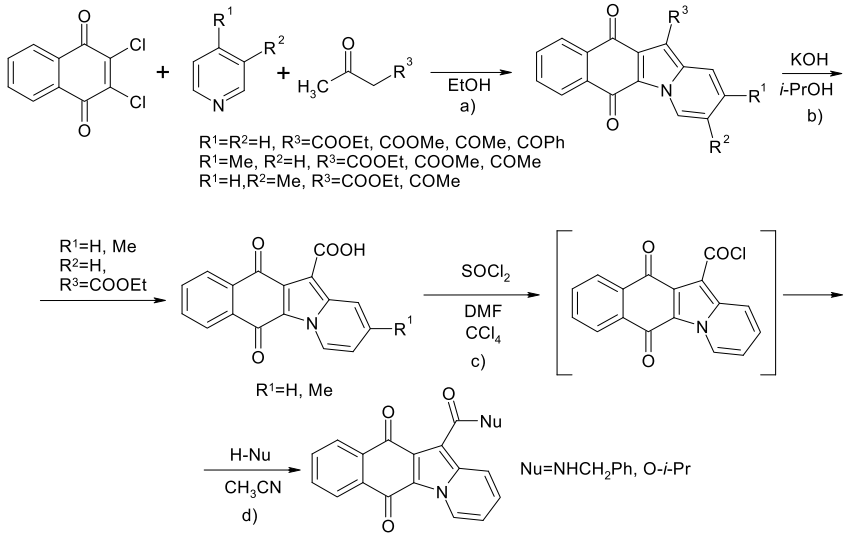

Table 6. MIC Determination and Susceptibility to F1414−1444 Analogues

	MIC$_{99}$ (μM)		
Strain name	F1414-1438	11626157	11626159
	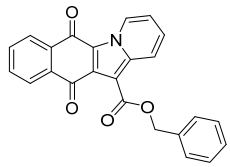	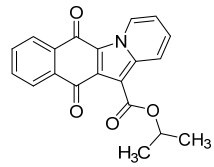	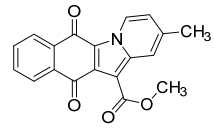
Erdman	1.56	1.56	5.1
DBPI1	20.2	10.2	20.1
DBPI2	15.3	12.5	22.3
DBPI3	15.5	12.2	22.2
DBPI4	40.2	12.6	21.4
DBPI4::pMV*E_0374*	1.7	1.54	5.6

Another highly upregulated gene that has been reported to be involved in drug resistance is *rv0560c*, encoding a methyltransferase, which *N*-methylates pyrido-benzimidazoles, thus abrogating their bactericidal activity.[46] The neighboring gene *rv0559c* was also upregulated by 11626157, and this encodes a secreted protein of unknown function. Overproduction of Rv0560c occurs following exposure of *M. tuberculosis* to a range of drugs and inhibitors, including salicylate and para-amino-salicylate,[47] membrane depolarizers (carbonyl cyanide *m*-chlorophenyl hydrazone, valinomycin, or dinitrophenol), the respiratory inhibitors chlorpromazine and thioridazine, and the detergent SDS.[46,47]

Expression of a cluster of three genes (*rv3093c*, *rv3094c*, and *rv3095*) was downregulated by both DBPI compounds, and these code for an oxidoreductase, a protein of unknown function, and an HTH transcriptional regulator (Figure 3B).

Hit Expansion and Structure−Activity Relationship (SAR) Exploration. To probe the structure−activity relationship, 13 new DBPI analogues of F1414−1444 were synthesized by medicinal chemistry. For the SAR, we explored position 12 of the benzo[*f*]pyrido[1,2-*a*]indole scaffold and also changed protons in positions 2 and 3 to methyl groups. Scheme 1 outlines the synthetic route and the structures of the new analogues, and details of their antitubercular activity are presented in the Supporting Information Table S3. We found that esters generally have stronger antitubercular activity than acids. Changing oxygen in the carboxylic moiety to nitrogen (11626154) or elimination of this oxygen from the structure leads to complete loss of activity probably due to formation of a strong hydrogen bond between the NH proton and 11-oxygen. The sequential introduction of Me (11626150), Et (11626149), and *i*-Pr (11626157) in the ester moiety revealed a good correlation between antibacterial activity and the alkyl size with the best activity found for the compound with the *i*-Pr substitution. Interaction of the Me group in positions 2 or 3 of 6,11-dioxobenzo[*f*]pyrido[1,2-*a*]indoles did not lead to a significant change in activity (Table S3).

https://dx.doi.org/10.1021/acsinfecdis.0c00531
ACS Infect. Dis. 2020, 6, 3015−3025

Data presented in Table 6 show that the two best characterized new derivatives also act by inhibition of IspQ (Rv0338c) as all four DBPI-resistant mutants of *M. tuberculosis* remained resistant, but susceptibility could be restored on complementing with the wild-type gene.

Drug-like Properties. To establish the drug-like properties of selected DBPI derivatives prior to testing in animal models we performed a series of *in vitro* ADME/T tests. Clearance was measured using the microsomal stability assay with a pool of human microsomes from 50 donors. Under these controlled conditions, clearance was found to be low to medium (Table 7). Furthermore, none of the DBPI compounds showed significant toxicity for HepG2 cells, and all were found to be nonmutagenic using the SOS-chromotest. Consistent with this, neither F1414−1444 nor 1438 were found to intercalate into DNA using electrophoretic mobility shift assays.

Table 7. Microsomal Stability Assay and Cytotoxicity

compound[a]	CLint (μL/min/mg)	clearance category	HepG2 TD_{50} (μM)[c]
F1414−1444	5.50	medium	44.3
F1414−1438	5.36	medium	40.0
11626157	1.59	low	NT
11626159	14.78[b]	medium	NT
CBZ	4.82	low	NT
NIF	44.79	high	NT

[a]CBZ, carbamazepine (low clearance control); NIF, nifedipine (high clearance control). [b]With this molecule, depletion was also observed after 60 min in the control tubes containing microsomes but not containing the NADPH regeneration solution which was not taken into consideration during the evaluation of the CLint value. [c]NT, not tested.

CONCLUDING REMARKS

The aim of exploring new chemical space for tuberculosis drug discovery was successfully met thanks to the use of the NCCR diversity-oriented compound library for phenotypic screening. This strategy uncovered many hits that will be described elsewhere, and the DBPI series to our knowledge has never been associated with antitubercular activity in previous screens. The best DBPI compounds show a number of attractive features as their MIC is close to their MBC, they retain activity against nonreplicating tubercle bacilli, and act in the single digit micromolar range. Furthermore, although orthologues of their target, IspQ, are present in numerous actinobacteria, the range of activity of DBPI is restricted to tubercle bacilli, which is a desirable feature. The early ADME/T properties encourage further testing in zebrafish or murine models of tuberculosis, and synthesis is currently being scaled up for this purpose. Upon investigating the structure−activity relationship, it was observed that the dioxo moiety was critical for activity, thus directing future SAR modifications to other components of the DBPI scaffold.

We present strong evidence for IspQ, a membrane-bound, putative iron−sulfur-binding reductase being the primary target of DBPI compounds. More than 20 years after the publication of the genome sequence of *M. tuberculosis* H37Rv,[48] we provide proof for an essential role for this protein and the first clue to its role by means of chemical biology. Its precise function remains unclear, but there are strong hints from the structural model, sequence similarities, gene expression profiling, and regulation studies that the protein, with its two Fe−S centers, might serve as a heterodisulfide reductase, and a role in electron transport is to be expected. From the drug development standpoint, this is encouraging because some of the most impressive progress in clinical trials has been made with drug candidates that inhibit ATP and energy production as exemplified by bedaquiline[8] and telacebec.[12] An additional desirable aspect for drug development is the prediction that the active site of the IspQ protein is predicted to be located in the periplasm, so inhibitors will not need to cross the plasma membrane to achieve their therapeutic effect. It is noteworthy that the active sites of three promiscuous tuberculosis drug targets, DprE1, MmpL3, and QcrB, are all directly accessible from the periplasm.[13,49]

Finally, a membrane-associated oxidoreductase complex, comprising the superoxide-detoxifier, SodA, the integral membrane protein, DoxX, and the thiol-oxidoreductase, SseA, was recently found to link radical detoxification with cytosolic thiol homeostasis.[40] It is conceivable that IspQ could play a similar role by sensing redox changes or perturbation of the activity of electron transport chains, but more work is required to test this hypothesis.

METHODS

NCCR Library. The NCCR library screened in this work is composed of 67,393 commercially available molecules ordered from Life Chemicals, Enamine and ChemDiv. The biggest set in the library with 53 620 molecules comprises diverse representatives of chemical space. On average six molecules represent one cluster enriched with 3D structures and sp3 centers. The rest of the library is composed of synthetic molecules designed and selected by using all commercially available natural products and derivatives as reference.

Bacterial Culture Condition. Culture conditions of *M. tuberculosis* strains such as Erdman, H37Rv (ATCC25618), clinical isolates, and other laboratory strains are described in the Supporting Information.

Screening the NCCR Library. Primary screening and dose−response determination were carried out in 384-well plates in duplicate using the resazurin reduction microtiter assay (REMA) as previously described.[15] Description of the instruments, materials, concentrations, and volumes used in the HTS screening are detailed in the Supporting Information.

Toxicity Assay. HepG2 human hepatocarcinoma cells were used for studying the toxicity of the investigated molecules. The Supporting Information contains more details.

Genotoxicity Assay. The genotoxicity of the compounds was evaluated by the SOS-chromotest on LB-agar plates.[17]

Determination of Minimal Bactericidal Concentration (MBC). To determine the minimal bactericidal concentration (MBC_{99}) of F1414−1444 *Mtb* Erdman cells (100 μL of OD_{600} 0.0001 in complete 7H9 medium) were treated with different compound concentrations (1/2XMIC-16XMIC). Treated and untreated bacteria were incubated at 37 °C during 7 and 14 d. After this time, 50 μL of undiluted and serially diluted cells were plated on 7H10 agar plates and incubated for 3 weeks at 37 °C, and the number of CFU determined for each plate where growth was observed. The compound concentration, where the CFU was lower than or equal to 99% of the CFU for the nontreated control, was considered as the MBC_{99}.

Resistant Mutant Isolation and Genomics. To isolate resistant mutants, *Mtb* Erdman (3×10^7 bacteria) were plated

https://dx.doi.org/10.1021/acsinfecdis.0c00531
ACS Infect. Dis. 2020, 6, 3015−3025

on Middlebrook 7H10 plates containing compounds at concentrations of 3×, 6×, 10×, 20×, and 50× of the MIC previously determined in liquid medium. Selected individual colonies were resuspended in 20 μL of 7H9 and restreaked on 7H10 plates containing the same concentration of compound from which they were isolated. Two to four colonies from each parent colony were then resuspended in 1 mL of complete 7H9 and incubated for 1 week at 37 °C without shaking. Then, the suspension was transferred to 5 mL of complete 7H9 medium, and the bacteria were grown to logarithmic phase to perform the REMA assay to test their dose−response to the compound. The susceptibility pattern of individual colonies was compared to that of the Erdman WT strain. Genomic DNA of the WT and mutant strains was sequenced on Illumina MiSeq/HiSeq instruments and reads processed as detailed in the Supporting Information.

Overexpression. To validate the putative drug target of the compound, the empty pMV261 vector and its pMVE_0374 construct were both transformed into the parental Erdman strain and its four representative DBPI-resistant mutants. The open reading frame of *ERDMAN_0374* was amplified from *Mtb* Erdman genomic DNA by PCR using a primer pair Rv0338c-FWD-*Bam*HI 5′TTAGGATCCAGTGACCACGCAAACGCTC 3′ and Rv0338c-REV-*Hpa*I2 5′AATGTTAACTCAGCGTTTGCCCGGTGGACG 3′ to clone them into pMV261.[50] The constructs were transformed into Erdman WT, and respective mutant strains and transformants were selected on 7H10 plates containing 25 μg/mL kanamycin. The total RNA was extracted by standard methods, and the overexpression of the genes was verified by real-time reverse transcription-PCR (RT-PCR) using the primer pairs Rv0338c_qPCR_F 5′ TTGTGGTCATGTGTGACCTG 3′and Rv0338c_qPCR_R 5′ TTCTTGAACAGCACCGACAG 3′. The dose−response to the compound was tested for at least two clones overexpressing each of the genes of interest, in comparison with the parent WT or mutant strains alone, and carrying the empty pMV261 plasmid.

Transcriptomics. Briefly, *M. tuberculosis* H37Rv was cultured to exponential phase ($OD_{600\ nm}$ 0.5) and exposed for 6 h to DMSO, as a control, and to either F1414−1444 or 11626157 (10 and 30 μM). Each sample was independently prepared in triplicate. Total RNA was extracted using hot phenol, and RNA integrity was evaluated by Bioanalyzer profiling. Ribosomal RNA was depleted using the QIAseq FastSelect -5S/16S/23S QIAGEN kit, and libraries were prepared using the TruSeq Stranded mRNA Library Preparation kit (Illumina). Sequencing was performed on the NextSeq500 WGS system at the Biomics platform (Institut Pasteur). Data were processed, and alignment and annotation were done using Bowtie;[51] the quality control (QC) report, the count expression table, and the differential analysis were obtained using DESeq2 and SARTools (1.7.0). A more extensive account of the methods used may be found in the Supporting Information.

Metabolic Stability Assay (Human Microsomal CLint). To study the metabolic stability of the molecule, human liver microsomes pooled from 50 donors were used as described in the Supporting Information.

■ ASSOCIATED CONTENT

Supporting Information

The Supporting Information is available free of charge at https://pubs.acs.org/doi/10.1021/acsinfecdis.0c00531.

Details of methods used, three tables, and six figures (PDF)

XLSX Table presents Transcriptome analysis following DBPI exposure (XLSX)

■ AUTHOR INFORMATION

Corresponding Author

Stewart T. Cole − *Global Health Institute, Ecole Polytechnique Fédérale de Lausanne, CH-1015 Lausanne, Switzerland; Microbial Individuality and Infection, Institut Pasteur, 75015 Paris, France;* orcid.org/0000-0003-1400-5585; Email: stewart.cole@pasteur.fr

Authors

Rita Székely − *Global Health Institute, Ecole Polytechnique Fédérale de Lausanne, CH-1015 Lausanne, Switzerland*

Monica Rengifo-Gonzalez − *Institute of Chemical Sciences and Engineering, Ecole Polytechnique Fédérale de Lausanne, CH-1015 Lausanne, Switzerland*

Vinayak Singh − *MRC/NHLS/UCT Molecular Mycobacteriology Research Unit & DST/NRF Centre of Excellence for Biomedical TB Research, Institute of Infectious Disease and Molecular Medicine & Department of Pathology, University of Cape Town, Cape Town 7701, South Africa;* orcid.org/0000-0001-9002-2489

Olga Riabova − *FRC Fundamentals of Biotechnology, Russian Academy of Science, 119071 Moscow, Russian Federation*

Andrej Benjak − *Global Health Institute, Ecole Polytechnique Fédérale de Lausanne, CH-1015 Lausanne, Switzerland*

Jérémie Piton − *Global Health Institute, Ecole Polytechnique Fédérale de Lausanne, CH-1015 Lausanne, Switzerland*

Mena Cimino − *Microbial Individuality and Infection, Institut Pasteur, 75015 Paris, France*

Etienne Kornobis − *Biomics, C2RT and Hub Bioinformatique et Biostatistique, USR 3756 CNRS, Institut Pasteur, 75015 Paris, France*

Valerie Mizrahi − *MRC/NHLS/UCT Molecular Mycobacteriology Research Unit & DST/NRF Centre of Excellence for Biomedical TB Research, Institute of Infectious Disease and Molecular Medicine & Department of Pathology, University of Cape Town, Cape Town 7701, South Africa;* orcid.org/0000-0003-4824-9115

Kai Johnsson − *Institute of Chemical Sciences and Engineering, Ecole Polytechnique Fédérale de Lausanne, CH-1015 Lausanne, Switzerland*

Giulia Manina − *Microbial Individuality and Infection, Institut Pasteur, 75015 Paris, France*

Vadim Makarov − *FRC Fundamentals of Biotechnology, Russian Academy of Science, 119071 Moscow, Russian Federation*

Complete contact information is available at: https://pubs.acs.org/10.1021/acsinfecdis.0c00531

Author Contributions

⬡R.S. and M.R. contributed equally and executed most of the experiments. R.S., V.S., G.M., K.J., V. Mi., V. Ma., and S.T.C. conceived and designed the experiments. O.R. synthesized compounds. V.S. constructed and analyzed cKD mutants. A.B.

performed genome analysis and provided bioinformatics support. J.P. constructed structural models. M.C., E.K., and G.M. performed RNA-Seq analysis. R.S. and S.T.C. wrote the manuscript, to which all authors contributed comments before approval of the final version.

Notes

The authors declare no competing financial interest.

■ ACKNOWLEDGMENTS

We thank Julien Bortoli Chapalay, Damiano Banfi, Antoine Gibelin, and Gerardo Turcatti from EPFL's Biomolecular Screening Facility for help with screening and compound management; Valérie Briolat and Marc Monot from the Institut Pasteur Biomics Platform for RNA-Seq support; and Priscille Brodin, Tony Maxwell, Claudia Sala, and Anthony Vocat of the MM4TB consortium for advice and technical support. This work was funded by the European Community's Seventh Framework Programme (MM4TB Grant 260872), the European Commission Marie Curie Fellowship (PIEF-GA-2012-327219 to R.S.), the Ministry of Education and Science of the Russian Federation (Agreement No. 14.616.21.0065; unique identifier RFMEFI61616X006.), grant VEGA (1/0284/15), and France Génomique (ANR-10-INBS-09-09).

■ ABBREVIATIONS USED

ADME/T, absorption distribution metabolism excretion/toxicity; ATc, anhydrotetracycline; BDQ, bedaquiline; CBZ, carbamazepine; CFZ, clofazimine; CFU, colony-forming units; DBPI, dioxo-dihydrobenzo-pyridoindole; INH, isoniazid; MIC_{99}, minimal inhibitory concentration leading to 99% growth inhibition; NIF, nifedipine; NTM, nontuberculous mycobacterial; REMA, resazurin microtiter assay; SNP, single nucleotide polymorphisms; STR, streptomycin; WGS, whole genome sequencing

■ REFERENCES

(1) WHO. *Global Tuberculosis Report 2018*; Geneva, 2018.

(2) Tameris, M. D., Hatherill, M., Landry, B. S., Scriba, T. J., Snowden, M. A., Lockhart, S., Shea, J. E., McClain, J. B., Hussey, G. D., Hanekom, W. A., Mahomed, H., and McShane, H. (2013) MVA85A 020 Trial Study Team. Safety and efficacy of MVA85A, a new tuberculosis vaccine, in infants previously vaccinated with BCG: a randomised, placebo-controlled phase 2b trial. *Lancet 381*, 1021−1028.

(3) Zumla, A., Nahid, P., and Cole, S. T. (2013) Advances in the development of new tuberculosis drugs and treatment regimens. *Nat. Rev. Drug Discovery 12*, 388−404.

(4) Zumla, A. I., Gillespie, S. H., Hoelscher, M., Philips, P. P., Cole, S. T., Abubakar, I., McHugh, T. D., Schito, M., Maeurer, M., and Nunn, A. J. (2014) New antituberculosis drugs, regimens, and adjunct therapies: needs, advances, and future prospects. *Lancet Infect. Dis. 14*, 327−340.

(5) Van Deun, A., Maug, A. K., Salim, M. A., Das, P. K., Sarker, M. R., Daru, P., and Rieder, H. L. (2010) Short, highly effective, and inexpensive standardized treatment of multidrug-resistant tuberculosis. *Am. J. Respir. Crit. Care Med. 182*, 684−692.

(6) Evans, J. C., and Mizrahi, V. (2018) Priming the tuberculosis drug pipeline: new antimycobacterial targets and agents. *Curr. Opin. Microbiol. 45*, 39−46.

(7) Brodin, P., and Christophe, T. (2011) High-content screening in infectious diseases. *Curr. Opin. Chem. Biol. 15*, 534−539.

(8) Andries, K., Verhasselt, P., Guillemont, J., Gohlmann, H. W., Neefs, J. M., Winkler, H., Van Gestel, J., Timmerman, P., Zhu, M., Lee, E., Williams, P., de Chaffoy, D., Huitric, E., Hoffner, S., Cambau, E., Truffot-Pernot, C., Lounis, N., and Jarlier, V. (2005) A diarylquinoline drug active on the ATP synthase of Mycobacterium tuberculosis. *Science 307*, 223−227.

(9) Stover, C. K., Warrener, P., VanDevanter, D. R., Sherman, D. R., Arain, T. M., Langhorne, M. H., Anderson, S. W., Towell, J. A., Yuan, Y., McMurray, D. N., Kreiswirth, B. N., Barry, C. E., and Baker, W. R. (2000) A small-molecule nitroimidazopyran drug candidate for the treatment of tuberculosis. *Nature 405*, 962−966.

(10) Matsumoto, M., Hashizume, H., Tomishige, T., Kawasaki, M., Tsubouchi, H., Sasaki, H., Shimokawa, Y., and Komatsu, M. (2006) OPC-67683, a nitro-dihydro-imidazooxazole derivative with promising action against tuberculosis in vitro and in mice. *PLoS Med. 3*, No. e466.

(11) Working Group on New TB Drugs. Clinical Pipeline. http://www.newtbdrugs.org/pipeline/clinical (accessed September 5, 2020).

(12) Pethe, K., Bifani, P., Jang, J., Kang, S., Park, S., Ahn, S., Jiricek, J., Jung, J., Jeon, H. K., Cechetto, J., Christophe, T., Lee, H., Kempf, M., Jackson, M., Lenaerts, A. J., Pham, H., Jones, V., Seo, M. J., Kim, Y. M., Seo, M., Seo, J. J., Park, D., Ko, Y., Choi, I., Kim, R., Kim, S. Y., Lim, S., Yim, S. A., Nam, J., Kang, H., Kwon, H., Oh, C. T., Cho, Y., Jang, Y., Kim, J., Chua, A., Tan, B. H., Nanjundappa, M. B., Rao, S. P., Barnes, W. S., Wintjens, R., Walker, J. R., Alonso, S., Lee, S., Kim, J., Oh, S., Oh, T., Nehrbass, U., Han, S. J., No, Z., Lee, J., Brodin, P., Cho, S. N., Nam, K., and Kim, J. (2013) Discovery of Q203, a potent clinical candidate for the treatment of tuberculosis. *Nat. Med. 19*, 1157−1160.

(13) Cole, S. T. (2016) Inhibiting Mycobacterium tuberculosis within and without. *Philos. Trans. R. Soc., B 371* (1707), 20150506.

(14) Swiss National Centre of Competence in Research - Chemical Biology. https://nccr-chembio.ch/ (accessed September 6, 2020)..

(15) Palomino, J. C., Martin, A., Camacho, M., Guerra, H., Swings, J., and Portaels, F. (2002) Resazurin microtiter assay plate: Simple and inexpensive method for detection of drug resistance in Mycobacterium tuberculosis. *Antimicrob. Agents Chemother. 46* (8), 2720−2722.

(16) Zhang, M., Sala, C., Hartkoorn, R. C., Dhar, N., Mendoza-Losana, A., and Cole, S. T. (2012) Streptomycin-Starved Mycobacterium tuberculosis 18b, a Drug Discovery Tool for Latent Tuberculosis. *Antimicrob. Agents Chemother. 56* (11), 5782−5789.

(17) Quillardet, P., Huisman, O., D'Ari, R., and Hofnung, M. (1982) SOS chromotest, a direct assay of induction of an SOS function in Escherichia coli K-12 to measure genotoxicity. *Proc. Natl. Acad. Sci. U. S. A. 79*, 5971−5975.

(18) Franzblau, S. G., DeGroote, M. A., Cho, S. H., Andries, K., Nuermberger, E., Orme, I. M., Mdluli, K., Angulo-Barturen, I., Dick, T., Dartois, V., and Lenaerts, A. J. (2012) Comprehensive analysis of methods used for the evaluation of compounds against Mycobacterium tuberculosis. *Tuberculosis 92*, 453−488.

(19) Benjak, A., Uplekar, S., Zhang, M., Piton, J., Cole, S. T., and Sala, C. (2016) Genomic and transcriptomic analysis of the streptomycin-dependent Mycobacterium tuberculosis strain 18b. *BMC Genomics 17* (190), 1 DOI: 10.1186/s12864-016-2528-2.

(20) Griffin, J. E., Gawronski, J. D., Dejesus, M. A., Ioerger, T. R., Akerley, B. J., and Sassetti, C. M. (2011) High-resolution phenotypic profiling defines genes essential for mycobacterial growth and cholesterol catabolism. *PLoS Pathog. 7* (9), No. e1002251.

(21) Tuberculist. https://mycobrowser.epfl.ch/ (accessed September 3, 2020).

(22) Singh, V., Donini, S., Pacitto, A., Sala, C., Hartkoorn, R. C., Dhar, N., Keri, G., Ascher, D. B., Mondesert, G., Vocat, A., Lupien, A., Sommer, R., Vermet, H., Lagrange, S., Buechler, J., Warner, D. F., McKinney, J. D., Pato, J., Cole, S. T., Blundell, T. L., Rizzi, M., and Mizrahi, V. (2017) The Inosine Monophosphate Dehydrogenase, GuaB2, Is a Vulnerable New Bactericidal Drug Target for Tuberculosis. *ACS Infect. Dis. 3*, 5−17.

(23) Saini, V., Farhana, A., Glasgow, J. N., and Steyn, A. J. (2012) Iron sulfur cluster proteins and microbial regulation: implications for understanding tuberculosis. *Curr. Opin. Chem. Biol. 16* (1−2), 45−53.

(24) Kelley, L. A., Mezulis, S., Yates, C. M., Wass, M. N., and Sternberg, M. J. (2015) The Phyre2 web portal for protein modeling, prediction and analysis. *Nat. Protoc. 10*, 845−858.
(25) Bertero, M. G., Rothery, R. A., Boroumand, N., Palak, M., Blasco, F., Ginet, N., Weiner, J. H., and Strynadka, N. C. (2005) Structural and biochemical characterization of a quinol binding site of Escherichia coli nitrate reductase A. *J. Biol. Chem. 280*, 14836−14843.
(26) Wagner, T., Koch, J., Ermler, U., and Shima, S. (2017) Methanogenic heterodisulfide reductase (HdrABC-MvhAGD) uses two noncubane [4Fe-4S] clusters for reduction. *Science 357*, 699−703.
(27) Singh, P., Benjak, A., Schuenemann, V. J., Herbig, A., Avanzi, C., Busso, P., Nieselt, K., Krause, J., Vera-Cabrera, L., and Cole, S. T. (2015) Insight into the evolution and origin of leprosy bacilli from the genome sequence of Mycobacterium lepromatosis. *Proc. Natl. Acad. Sci. U. S. A. 112*, 4459−4464.
(28) Benjak, A., Avanzi, C., Singh, P., Loiseau, C., Girma, S., Busso, P., Fontes, A. N. B., Miyamoto, Y., Namisato, M., Bobosha, K., Salgado, C. G., da Silva, M. B., Bouth, R. C., Frade, M. A. C., Filho, F. B., Barreto, J. G., Nery, J. A. C., Buhrer-Sekula, S., Lupien, A., Al-Samie, A. R., Al-Qubati, Y., Alkubati, A. S., Bretzel, G., Vera-Cabrera, L., Sakho, F., Johnson, C. R., Kodio, M., Fomba, A., Sow, S. O., Gado, M., Konate, O., Stefani, M. M. A., Penna, G. O., Suffys, P. N., Sarno, E. N., Moraes, M. O., Rosa, P. S., Baptista, I., Spencer, J. S., Aseffa, A., Matsuoka, M., Kai, M., and Cole, S. T. (2018) Phylogenomics and antimicrobial resistance of the leprosy bacillus Mycobacterium leprae. *Nat. Commun. 9* (1), 352.
(29) Stinear, T. P., Seemann, T., Harrison, P. F., Jenkin, G. A., Davies, J. K., Johnson, P. D., Abdellah, Z., Arrowsmith, C., Chillingworth, T., Churcher, C., Clarke, K., Cronin, A., Davis, P., Goodhead, I., Holroyd, N., Jagels, K., Lord, A., Moule, S., Mungall, K., Norbertczak, H., Quail, M. A., Rabbinowitsch, E., Walker, D., White, B., Whitehead, S., Small, P. L., Brosch, R., Ramakrishnan, L., Fischbach, M. A., Parkhill, J., and Cole, S. T. (2008) Insights from the complete genome sequence of Mycobacterium marinum on the evolution of Mycobacterium tuberculosis. *Genome Res. 18*, 729−741.
(30) Malen, H., Pathak, S., Softeland, T., de Souza, G. A., and Wiker, H. G. (2010) Definition of novel cell envelope associated proteins in Triton X-114 extracts of Mycobacterium tuberculosis H37Rv. *BMC Microbiol. 10*, 132.
(31) de Souza, G. A., Leversen, N. A., Malen, H., and Wiker, H. G. (2011) Bacterial proteins with cleaved or uncleaved signal peptides of the general secretory pathway. *J. Proteomics 75*, 502−510.
(32) Rodriguez, G. M., Voskuil, M. I., Gold, B., Schoolnik, G. K., and Smith, I. (2002) ideR, An essential gene in mycobacterium tuberculosis: role of IdeR in iron-dependent gene expression, iron metabolism, and oxidative stress response. *Infect. Immun. 70*, 3371−3381.
(33) Boshoff, H. I., Myers, T. G., Copp, B. R., McNeil, M. R., Wilson, M. A., and Barry, C. E., 3rd (2004) The transcriptional responses of Mycobacterium tuberculosis to inhibitors of metabolism: novel insights into drug mechanisms of action. *J. Biol. Chem. 279* (38), 40174−40184.
(34) Smyth, A., and Gordon, S. V. (2018) Molecular virulence mechanisms of *Mycobacterium bovis*. In *Bovine tuberculosis*, Chambers, M., Gordon, S., Olea-Popolka, F., and Barrow, P., Eds. CABI: 2018; pp 106−121, Wallingford, Oxfordshire, U.K.; Boston, MA, United States.
(35) Sachdeva, P., Misra, R., Tyagi, A. K., and Singh, Y. (2010) The sigma factors of Mycobacterium tuberculosis: regulation of the regulators. *FEBS J. 277*, 605−626.
(36) Zhou, P., Wang, X., Zhao, Y., Yuan, W., and Xie, J. (2018) Sigma factors mediated signaling in Mycobacterium tuberculosis. *Future Microbiol. 13*, 231−240.
(37) Tiwari, S., van Tonder, A. J., Vilcheze, C., Mendes, V., Thomas, S. E., Malek, A., Chen, B., Chen, M., Kim, J., Blundell, T. L., Parkhill, J., Weinrick, B., Berney, M., and Jacobs, W. R., Jr. (2018) Arginine-deprivation-induced oxidative damage sterilizes Mycobacterium tuberculosis. *Proc. Natl. Acad. Sci. U. S. A. 115*, 9779−9784.
(38) Lee, B. S., Sviriaeva, E., and Pethe, K. (2020) Targeting the cytochrome oxidases for drug development in mycobacteria. *Prog. Biophys. Mol. Biol. 152*, 45−54.
(39) Padilla-Benavides, T., McCann, C. J., and Arguello, J. M. (2013) The mechanism of Cu+ transport ATPases: interaction with CU+ chaperones and the role of transient metal-binding sites. *J. Biol. Chem. 288*, 69−78.
(40) Nambi, S., Long, J. E., Mishra, B. B., Baker, R., Murphy, K. C., Olive, A. J., Nguyen, H. P., Shaffer, S. A., and Sassetti, C. M. (2015) The Oxidative Stress Network of Mycobacterium tuberculosis Reveals Coordination between Radical Detoxification Systems. *Cell Host Microbe 17*, 829−837.
(41) Bottai, D., Frigui, W., Sayes, F., Di Luca, M., Spadoni, D., Pawlik, A., Zoppo, M., Orgeur, M., Khanna, V., Hardy, D., Mangenot, S., Barbe, V., Medigue, C., Ma, L., Bouchier, C., Tavanti, A., Larrouy-Maumus, G., and Brosch, R. (2020) TbD1 deletion as a driver of the evolutionary success of modern epidemic Mycobacterium tuberculosis lineages. *Nat. Commun. 11*, 684.
(42) Arumugam, P., Shankaran, D., Bothra, A., Gandotra, S., and Rao, V. (2019) The MmpS6-MmpL6 Operon Is an Oxidative Stress Response System Providing Selective Advantage to Mycobacterium tuberculosis in Stress. *J. Infect. Dis. 219*, 459−469.
(43) Hartkoorn, R. C., Uplekar, S., and Cole, S. T. (2014) Cross-resistance between clofazimine and bedaquiline through upregulation of MmpL5 in Mycobacterium tuberculosis. *Antimicrob. Agents Chemother. 58*, 2979−2981.
(44) Andries, K., Villellas, C., Coeck, N., Thys, K., Gevers, T., Vranckx, L., Lounis, N., de Jong, B. C., and Koul, A. (2014) Acquired resistance of Mycobacterium tuberculosis to bedaquiline. *PLoS One 9*, No. e102135.
(45) Milano, A., Pasca, M. R., Provvedi, R., Lucarelli, A. P., Manina, G., Ribeiro, A. L., Manganelli, R., and Riccardi, G. (2009) Azole resistance in Mycobacterium tuberculosis is mediated by the MmpS5-MmpL5 efflux system. *Tuberculosis 89*, 84−90.
(46) Warrier, T., Kapilashrami, K., Argyrou, A., Ioerger, T. R., Little, D., Murphy, K. C., Nandakumar, M., Park, S., Gold, B., Mi, J., Zhang, T., Meiler, E., Rees, M., Somersan-Karakaya, S., Porras-De Francisco, E., Martinez-Hoyos, M., Burns-Huang, K., Roberts, J., Ling, Y., Rhee, K. Y., Mendoza-Losana, A., Luo, M., and Nathan, C. F. (2016) N-methylation of a bactericidal compound as a resistance mechanism in Mycobacterium tuberculosis. *Proc. Natl. Acad. Sci. U. S. A. 113*, E4523−30.
(47) Schuessler, D. L., and Parish, T. (2012) The promoter of Rv0560c is induced by salicylate and structurally-related compounds in Mycobacterium tuberculosis. *PLoS One 7* (4), No. e34471.
(48) Cole, S. T., Brosch, R., Parkhill, J., Garnier, T., Churcher, C., Harris, D., Gordon, S. V., Eiglmeier, K., Gas, S., Barry, C. E., 3rd, Tekaia, F., Badcock, K., Basham, D., Brown, D., Chillingworth, T., Connor, R., Davies, R., Devlin, K., Feltwell, T., Gentles, S., Hamlin, N., Holroyd, S., Hornsby, T., Jagels, K., Krogh, A., McLean, J., Moule, S., Murphy, L., Oliver, K., Osborne, J., Quail, M. A., Rajandream, M. A., Rogers, J., Rutter, S., Seeger, K., Skelton, J., Squares, R., Squares, S., Sulston, J. E., Taylor, K., Whitehead, S., and Barrell, B. G. (1998) Deciphering the biology of Mycobacterium tuberculosis from the complete genome sequence. *Nature 393*, 537−544.
(49) Brecik, M., Centarova, I., Mukherjee, R., Kolly, G. S., Huszar, S., Bobovska, A., Kilacskova, E., Mokosova, V., Svetlikova, Z., Sarkan, M., Neres, J., Kordulakova, J., Cole, S. T., and Mikusova, K. (2015) DprE1 Is a Vulnerable Tuberculosis Drug Target Due to Its Cell Wall Localization. *ACS Chem. Biol. 10*, 1631−1636.
(50) Larsen, M. H., Vilcheze, C., Kremer, L., Besra, G. S., Parsons, L., Salfinger, M., Heifets, L., Hazbon, M. H., Alland, D., Sacchettini, J. C., and Jacobs, W. R., Jr. (2002) Overexpression of inhA, but not kasA, confers resistance to isoniazid and ethionamide in Mycobacterium smegmatis, M. bovis BCG and M. tuberculosis. *Mol. Microbiol. 46*, 453−466.
(51) Langmead, B., and Salzberg, S. L. (2012) Fast gapped-read alignment with Bowtie 2. *Nat. Methods 9*, 357−359.

https://dx.doi.org/10.1021/acsinfecdis.0c00531
ACS Infect. Dis. 2020, 6, 3015−3025